

Factors That Influence Electrical Resistivity Measurements in Cementitious Systems

Robert Spragg, Chiara Villani, Ken Snyder, Dale Bentz, Jeffrey W. Bullard, and Jason Weiss

The electrical resistivity of cement-based materials can be used in quality control or service life prediction as an indicator of the fluid transport properties of these materials. Although electrical tests have the advantage of being easy and rapid to perform, several key factors can influence the results: (a) specimen geometry, (b) specimen temperature, and (c) sample storage and conditioning. This paper addresses these issues and compares the measurements from several commercially available testing devices. First, the role of sample geometry is explained with the use of three common geometries: surface, uniaxial, and embedded electrodes. If the geometry is properly accounted for, measurements from different test geometries result in electrical resistivity values that are similar. Second, the role of sample temperature is discussed for both pore solution and uniaxial tests on cylinders. Third, the paper examines the importance of sample curing, storage, and conditioning. Sample storage and conditioning influence both the degree of hydration and the degree of saturation. The role of sample volume to solution volume is discussed, as this ratio may influence alkali leaching and pore solution conduction. This paper is intended to identify factors that influence the results of rapid electrical test measurements and to help identify areas of future research that are needed so that robust specifications and standard test methods can be developed. Standardization will enable electrical tests to provide rapid, accurate, repeatable measurements of concrete's electrical properties.

The electrical properties of cement-based materials have been investigated for nearly a century (1–3). One practical use of electrical measurements is the standard test commonly referred to as the rapid chloride permeability test. This test measures the charge passed in a saturated sample over time when a constant voltage is applied. Although it is widely used, the rapid chloride permeability test has a few shortcomings related to its relatively long sample preparation time; its destructive nature; and sample heating, which influences the results (4–7). Given these limitations, there is growing interest in developing nondestructive resistivity measurements to replace the rapid chloride permeability test. The benefit of resistivity tests is that they can be low cost, repeatable, and rapid to perform (6, 8, 9).

R. Spragg, C. Villani, and J. Weiss, School of Civil Engineering, Purdue University, 550 Stadium Mall Drive, West Lafayette, IN 47907-2051. K. Snyder, D. Bentz, and J. W. Bullard, Materials and Structural Systems Division, National Institute of Standards and Technology, 100 Bureau Drive, Stop 8615, Gaithersburg, MD 20899. Corresponding author: R. Spragg, rspragg@purdue.edu.

Transportation Research Record: Journal of the Transportation Research Board, No. 2342, Transportation Research Board of the National Academies, Washington, D.C., 2013, pp. 90–98.
DOI: 10.3141/2342-11

AASHTO and ASTM are in the process of developing standard test methods for surface resistivity testing, and a multiuser study was conducted to assess the variability of two rapid resistivity tests (8, 9). Although substantial research has focused on electrical methods over the past 30 years to describe material structure and transport properties, comparatively little research has focused on the role of sample conditioning and sample geometry (10–16). This paper highlights important features that may need to be captured in the ongoing development of standard test methods.

INFLUENCING FACTORS

Influence of Sample Geometry

Several sample geometries have been used to measure the electrical properties of concrete. This section describes these geometries and discusses how they can be related to one another. The most commonly used geometries are shown in Figure 1. The first geometry is referred to as surface resistivity (Figure 1a). The surface resistivity test uses a four-electrode configuration in which an alternating current is passed between the outer probes, and the voltage is measured between the inner probes. In this study a standard 100-mm-diameter \times 200-mm-long cylinder specimen was used with a probe spacing of 38 mm. The second geometry is typical of a uniaxial test, in which a set of plate electrodes is placed at the ends of a cylindrical specimen and used to measure the resistance through the cylinder (Figure 1b). This test was conducted using the testing procedure described by Spragg et al. (9). The third geometry evaluated in this study used a set of embedded stainless steel rods. A standard 150- \times 300-mm test cylinder was used with two embedded threaded rods as shown in Figure 1c and described by Castro et al. (17).

The tests highlighted in this study are based on measuring the electrical resistance between electrodes on a sample. This electrical resistance can be related to the geometry-independent property known as resistivity using the approach shown in Equation 1:

$$\rho = Rk \quad (1)$$

where

ρ = material resistivity,
 R = measured resistance, and
 k = geometry correction factor.

The geometry correction factor can be determined numerically (11, 18) or experimentally (9, 19) and is shown in Figure 1 for the geometries described above. In addition to these geometries, a wide

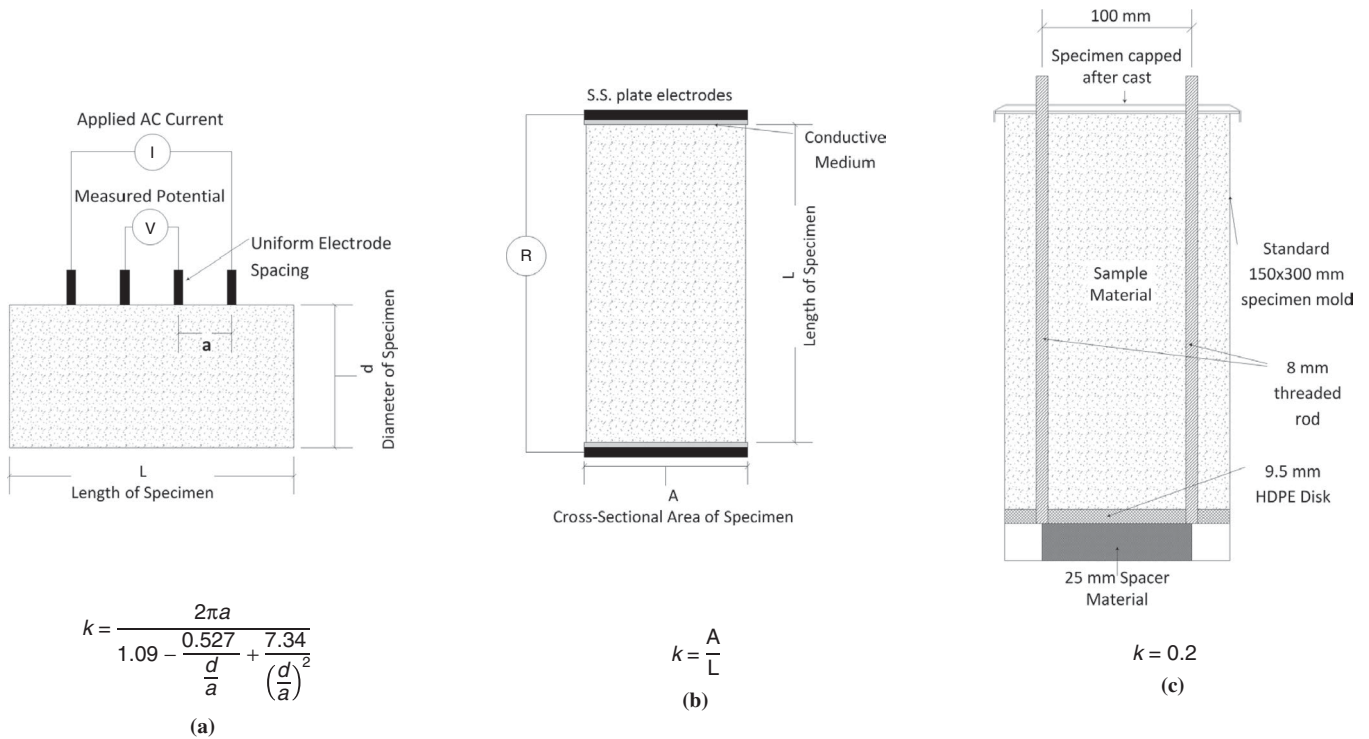


FIGURE 1 Testing geometries and geometry correction factor (k) for cylindrical specimens with (a) surface (k as shown is valid only for specimens with $d/a \leq 4.0$ and $L/a \geq 5.0$), (b) uniaxial, and (c) embedded electrode (k as shown is valid only for this specimen geometry) geometries (AC = alternating current; S.S. = stainless steel; HDPE = high-density polyethylene).

range of electrode geometries and specimen sizes can be used for this type of testing, provided the geometry factor can be determined, with examples provided in the literature (11, 19–21).

Influence of Sample Temperature

The temperature of the sample can substantially influence the measured resistivity (3, 22–25). An increase in the temperature of the sample results in an increase in the mobility of the ions in the pore solution and a decrease in measured resistivity. Although several approaches have been proposed to account for temperature, the correction investigated by the authors is a variation of the Arrhenius law, as shown in Equation 2:

$$\rho_{t-\text{ref}} = \rho_t \cdot \exp\left[\frac{E_{A-\text{cond}}}{R} \left(\frac{1}{T} - \frac{1}{T_{\text{ref}}}\right)\right] \quad (2)$$

where

$\rho_{t-\text{ref}}$ = resistivity (ohm · m) at reference temperature (23°C in the United States),

ρ_t = resistivity (ohm · m) at testing temperature,

$E_{A-\text{cond}}$ = activation energy of conduction (kJ/mol),

R = universal gas constant (8.314 J/[mol · K]),

T = testing temperature (K), and

T_{ref} = reference temperature (K) (23°C).

Although changes in temperature can influence the rate of hydration of cement-based materials, this correction is intended to account for the influence of temperature on the electrical measurements, and

hydration effects are dealt with separately (25). This work investigated the influence of temperature on both the pore solution and sample resistivities.

Influence of Sample Storage and Conditioning

Another important factor that can influence electrical measurements is how the samples are stored and conditioned. To best illustrate this approach, the Virtual Cement and Concrete Testing Laboratory model developed by the National Institute of Standards and Technology was used to simulate a mortar with a water-to-cement ratio of 0.42 with three curing conditions: (a) sealed during curing and testing, (b) sealed during curing and saturated during testing, and (c) saturated during curing and testing. Details on how these simulations were performed are available elsewhere (26, 27). Two primary factors influence this response: the degree of hydration of the cement and the degree of saturation of the sample.

The uniaxial mortar resistivity (ρ_c) values calculated from these simulations, normalized by the resistivity of the fluid in the pores (ρ_o), are shown in Figure 2. The sample that was sealed both during curing and testing had the greatest resistivity. The sample that was sealed during curing and saturated at the time of testing had the lowest resistivity. Although the pore structure and degree of hydration of both samples were the same, the difference can be explained by the moisture content (or degree of saturation) of the sample. An approach has been proposed to account for changes in resistivity in partially saturated concrete by using Equation 3 (27):

$$\rho^* = \rho \delta^{n-1+\delta} \quad (3)$$

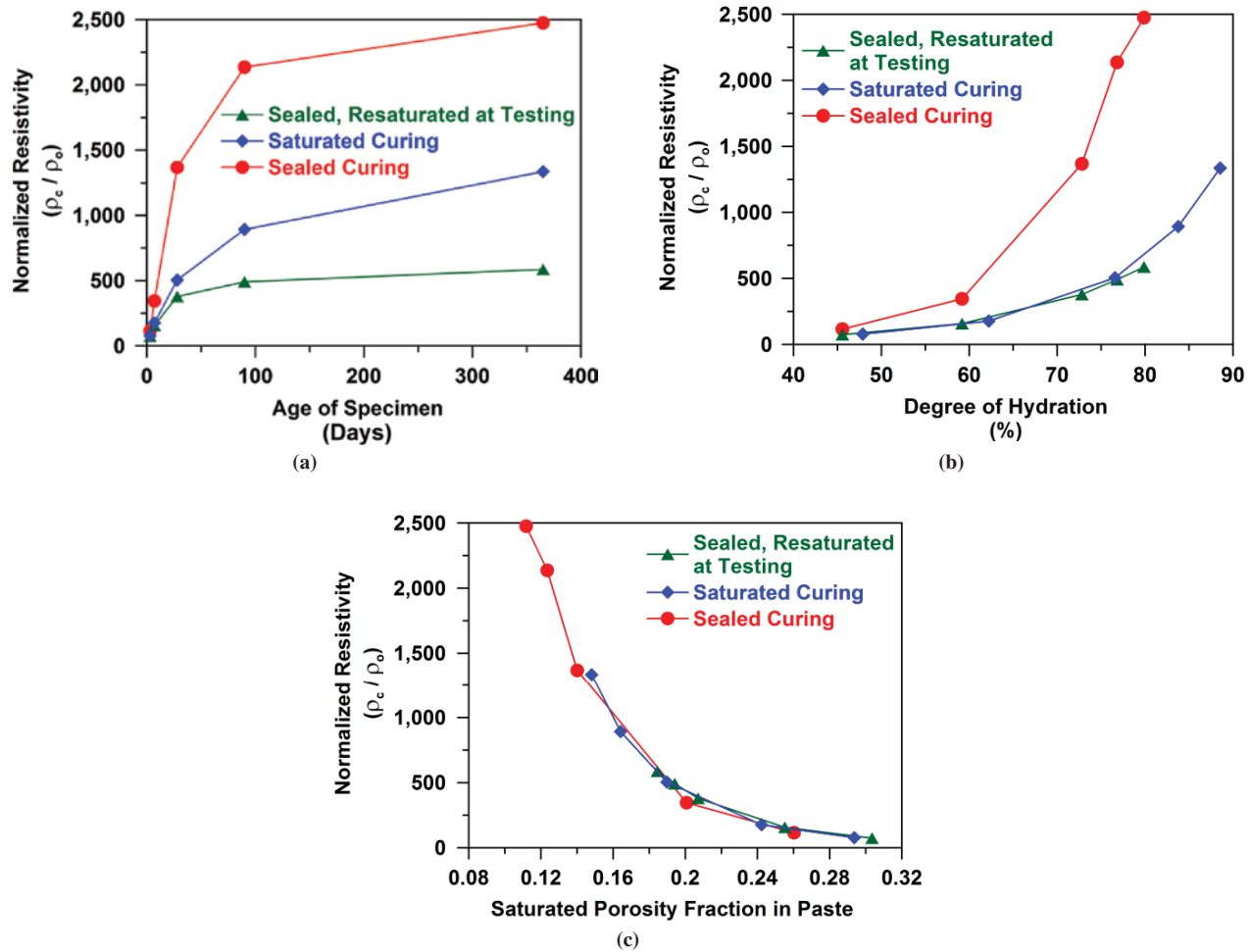


FIGURE 2 Virtual Cement and Concrete Testing Laboratory simulations of the same water-to-cement ratio (0.42) mortar mixture for normalized resistivity by (a) age of specimen, (b) degree of hydration, and (c) saturated porosity fraction in paste for three curing conditions (data are shown at 3, 7, 28, 90, and 365 days and are presented normalized by the resistivity of fluid in pores).

where

- ρ^* = resistivity at saturation,
- ρ = resistivity at given level of saturation S (which is between 0 and 1), and
- n = fitting parameter (saturation coefficient).

The parameter δ describes the ionic strength of the pore solution and how it changes during drying. For the mortar used in this study (the physical experiments), the degree of saturation was varied between 85% and 100%. It was observed that an exponent ($n - 1 + \delta$) of 4.15 best fit the data, which compares well with the data presented by Weiss et al. from the simulations (27).

Figure 2 also shows that the storage of samples in lime water resulted in a greater degree of hydration than that achieved in sealed samples. The data points in Figure 2b provide evidence that different degrees of hydration occurred in response to sample conditioning; Figure 2a presents these measurements at the same specimen age. The results suggest that storing a sample underwater in the lab may result in a substantially different degree of hydration than what may occur in a field structure. The sample that was continually saturated and the sample that was sealed and saturated at the time of testing had a similar resistivity for the same degree of hydration; however,

the continually saturated sample had a higher degree of hydration at the same age. In Figure 2c, these model results suggest that, for a given sample, resistivity at any degree of saturation can be estimated from a single measurement, given that the relative change in the pore solution conductivity can also be predicted. These models also suggest that resistivity measurements can be evaluated in terms of the fraction of saturated porosity in the paste, as shown in Figure 2c, with results similar to those reported by Weiss et al. (27).

It has been hypothesized that for samples cured under saturated lime water, the volume of solution in which the samples are stored can influence resistivity measurements. This influence may be caused by possible pore solution concentration or dilution via leaching. This work carefully investigated the influence of the volume of storage solution to sample size that was used for saturated lime-water curing.

MATERIALS

The samples were made with a mortar and a paste, each with a water-to-cement ratio of 0.42 by mass. The mortar mixture consisted of 55% aggregate by volume made with a fine aggregate with a specific gravity of 2.61 and an absorption capacity of 2.20% by dry mass. A

Type I ordinary portland cement with a Blaine fineness of $375 \text{ m}^2/\text{kg}$, a specific gravity of 3.17, and an estimated Bogue composition of 60% C_3S (tricalcium silicate), 10% C_2S (dicalcium silicate), 9% C_3A (tricalcium aluminate), and 10% C_4AF (tetracalcium aluminoferrite) by mass was used. The cement contained an alkali content of 0.35% Na_2O (sodium oxide) and 0.77% K_2O (potassium oxide). On the basis of the chemical composition, the ultimate theoretical heat release was calculated to be 512 J/g , using the tabulated heat of hydration of each Bogue phase (28, 29).

Samples were stored in a lime-saturated solution that was always used at a lime dosage rate of 3.0 g/L of solution to ensure a saturated solution. At saturation, the solubility of pure calcium hydroxide is 1.2 g/L of water.

EXPERIMENTAL EQUIPMENT USED FOR RESISTIVITY TESTING

Sample resistance was measured with four commercially available resistivity meters. Each meter used an alternating current, but operated at a different frequency. The Proceq Resipod was used for surface resistivity testing (Figure 1a) at a fixed probe tip spacing of 38 mm and uniaxial resistivity testing (Figure 1b) using the uniaxial resistivity testing kit available from Proceq, and operating at a frequency of 40 Hz. The M. C. Miller 400D was used in uniaxial resistivity testing (Figure 1b) at a frequency of 80 Hz. The uniaxial measurements (Figure 1b) using the RCON meter were performed at a single frequency (1 kHz), with the exception of the equivalent circuit model discussed below. To quantify the effect of a single frequency measurement, the Solatron 1260A impedance spectrometer across a frequency range of 1 Hz to 10 MHz was used.

EXPERIMENTAL RESULTS AND DISCUSSION

Corrections for Geometry

Measurements of electrical resistance were made on sealed specimens (i.e., specimens heat sealed in double plastic bags between testing); the results are shown in Figure 3a. When the appropriate correction for geometry was applied (using Equation 1 and values specified in

Figure 1) to calculate the electrical resistivity, the results obtained from different specimens of different geometries were quite comparable (Figure 3b).

It is interesting to note that a few of the early-age uniaxial measurements made with the Miller resistivity meter (hollow diamond symbols in Figure 3) show a much lower resistance. These lower measurements were traced to low battery levels. When the battery was replaced for a second set of experiments, the results were comparable with other experimental results. This unexpected occurrence, however, shows the value in having a standard, unchanging reference sample that can be used each day to confirm that the meter is working properly.

Pore Solution Contribution

The resistivity of the sealed mortar was measured and is plotted against the degree of hydration as determined from isothermal calorimeter measurements (Figure 4a) (30). Resistivity was nearly a linear function of the degree of hydration, which is similar to previously reported data (11, 17, 31).

The pore solution, which is the primary conducting phase in cement-based materials, has a resistivity several orders of magnitude lower than the solid and vapor phases (11). To study how the pore solution changes with hydration, the pore solution was extracted from paste specimens with a water-to-cement ratio of 0.42. Solutions were extracted at ages of 10 min and 1, 2, 3, 4, 5, 6, and 7 h while still in the fresh state by a Millipore pressure filtering system. The procedure used nitrogen gas at pressures up to 200 kPa (32). Extractions performed on hardened samples were conducted at ages of 1, 3, 5, and 7 days using a high-pressure die at pressures up to 380 MPa as described by Barneyback and Diamond (33). The extracted solutions were measured for resistivity using a pore solution cell described by Castro (30).

The experimentally measured pore solutions were compared with a model that was developed into an online tool by Bentz (<http://concrete.nist.gov/poresolnCalc.html>) (34, 35). This model predicts the electrical properties of the pore solution using only the masses of the water, cement, and supplementary materials; the chemical composition of those materials (i.e., their Na_2O , K_2O , and SiO_2 [silicon dioxide] mass percentages); and the estimated degree of hydration. The model estimates the composition of the pore solution and then evaluates the electrical properties of this pore solution.

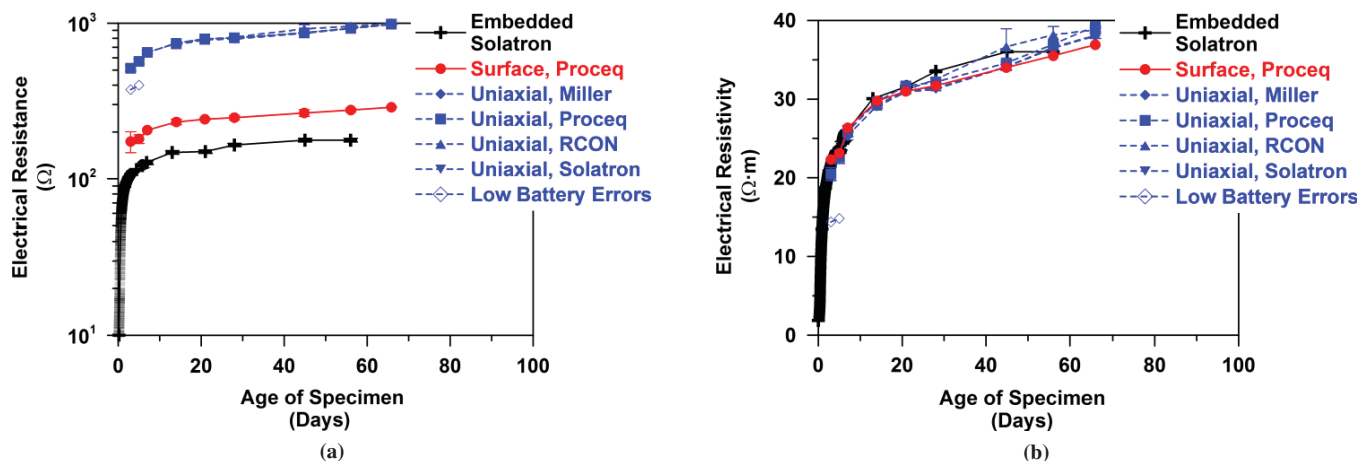


FIGURE 3 Measurements conducted on sealed mortar specimens with different geometries for (a) resistance and (b) resistivity (error bars represent standard deviation of three specimens).

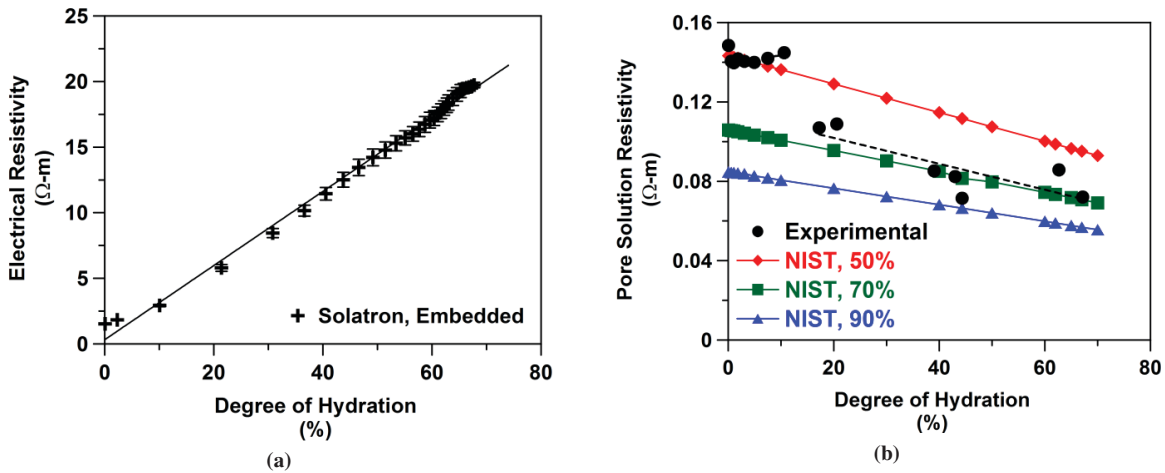


FIGURE 4 Resistivity measurements on (a) sealed mortar specimens (error bars represent standard deviation of three specimens) and (b) extracted pore solution compared with model results for different alkali dissolution percentages (NIST = National Institute of Standards and Technology).

One assumption, however, that has to be made in this model is the proportion of the alkalis that initially dissolves in the solution. Although a value of 75% is a typical default value that can be employed, assumed values of 50%, 70%, and 90% are shown in Figure 4b along with the experimental results. Initially, a value of 50% of the alkalis dissolving in solution appears appropriate; however, between a degree of hydration of 10% and 20%, this value suddenly increased to 70%. It is interesting that this increase appears to relate to the shoulder of the heat release curve that was observed for this system and that generally relates to the renewed reaction of the calcium aluminate phase of the cement. Several methods currently exist to rapidly assess pore solution resistivity, including pore solution extraction, estimation using an approach like the method on the National Institute of Standards and Technology website, and embedded sensors (11, 17). Research is ongoing to better understand the correlation between these results.

Influence of Temperature

Temperature can also influence the measured electrical response. For example, the resistivity measured using the same mature sample can differ by as much as 80% when the temperature of the sample fluctuates between 10°C and 45°C. This is primarily a result of the increased ionic mobility of the material’s pore solution and can be described using an Arrhenius approach (Equation 2).

The activation energy of conduction (E_{A-cond}) can be determined using the slope of a plot of the natural logarithm of resistivity and the inverse of temperature (Figure 5). The slope of the best-fit line is multiplied by the negative of the universal gas constant [$-8.314 J/(mol \cdot K)$] to determine the activation energy of conduction.

Figure 5 shows the results for mature mortar cylinders (closed symbols) and extracted pore solution (open symbols). The sealed specimens exhibited an activation energy of conduction of 23.4 ± 0.13 kJ/mol, the specimens stored with a volume-to-solution ratio of 2.0 exhibited an average value of 21.5 ± 0.08 kJ/mol, and the specimens stored with a solution-to-sample ratio of 11.4 exhibited a value of 19.9 ± 0.42 kJ/mol. Previously reported values for the activation energy of conduction in mortar specimens have included 18.7 ± 2.5 kJ/mol, values in excess of 20, and ranges of 16 to 30 kJ/mol

(11, 23, 25). The activation energy of conduction was also measured on pore solution extracted from specimens at ages of 12 and 24 h, resulting in values of 8.7 ± 0.18 kJ/mol and 7.7 ± 0.12 kJ/mol, respectively. Previously reported results for synthetic and extracted solutions have ranged from 8.98 to 13.8 kJ/mol (11, 17, 25).

As noted by Rajabipour, this difference between the measured activation energies of conduction obtained on extracted pore solution and uniaxial cylinders appears to suggest that the microstructure of a material can also influence these measurements (11). This difference may be partially caused by the confinement provided by the pore space, pore constriction, surface absorption effects, or changes in the pore fluid volume during heating and cooling. Additional work is needed to fully understand the reasons for these changes.

Influence of Sample Storage and Conditioning

The conduction of electrical current occurs primarily through the pore fluid in the cementitious system. Although the pore solution

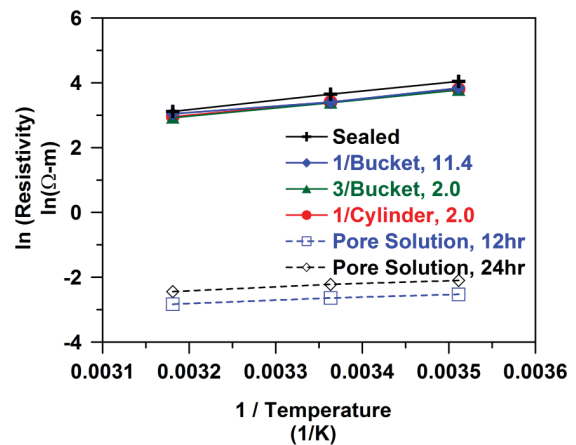


FIGURE 5 Activation energy of conduction measured on uniaxial samples (closed points) and extracted pore solution (hollow points) by electrical impedance spectroscopy (linear fits show an average R^2 of .996).

changes during hydration, it may also change if ions leach from the sample to the surrounding solution. A series of tests was conducted in which the ratios of the volumes of the lime-saturated solution to sample (Sol/Sam) varied (2.0 and 11.4). A Sol/Sam of 2.0 can be obtained when using a standard 100- × 200-mm testing specimen by using one specimen in a standard 150- × 300-mm mold or three samples in a 5-gal bucket. A Sol/Sam of 11.4 can be obtained by using a single specimen in a 5-gal bucket.

The samples were stored in a lime-saturated solution as described above and were monitored for electrical resistivity. The nominal resistivity of the lime-saturated solution was 12.6 Ω-m. The measured resistivity of the solution in the system in which Sol/Sam was 11.4 increased to a value of 16 Ω-m at approximately 2 weeks; it then began to decrease, reaching 13.8 Ω-m after 2 months. The measured resistivity of the solution in the system in which Sol/Sam was 2.0 decreased to a value of 2 Ω-m in approximately 1 week, and then slowly decreased to 1.3 Ω-m after 2 months. Initial data suggest this decrease was the result of ion leaching and dilution effects, but future research will investigate this change in more detail.

In addition to monitoring the resistivity of the solution, resistivity was measured on the sample with surface and uniaxial geometries at

a frequency of 40 Hz, and uniaxial resistivity was measured over a range of frequencies. Figure 6 shows the resistivity for the samples measured using the different storage conditions. The resistivity of the sealed sample was higher than the samples stored in the solution with a Sol/Sam of 2.0. This difference can be explained by the fact that the samples in solution have a higher degree of saturation.

The measurements on samples stored with a Sol/Sam of 11.4, in which the resistivity was measured at low frequency, more closely resemble the measurements conducted on sealed samples than on lime water-cured samples (Figure 6*b*). Testing at a variable frequency (Figure 6*c*) provided similar results for specimens stored in both Sol/Sam with less than 1% difference.

At ages up to 7 days, the surface resistivity measurements had more variability than the uniaxial measurements, as shown by standard deviations that are up to 2.7 times higher for surface measures of eight samples (Figure 6, *a* and *b*). At later ages the effect of storage solution volume seems to be reduced. This decreased variability can likely be attributed to the effects of leaching of surface alkalis in both solution volumes. The results obtained to date suggest that at later ages, the influence of storage solution volume on surface measurements and uniaxial measurements at variable frequencies (Figure 6, *a* and *c*) is

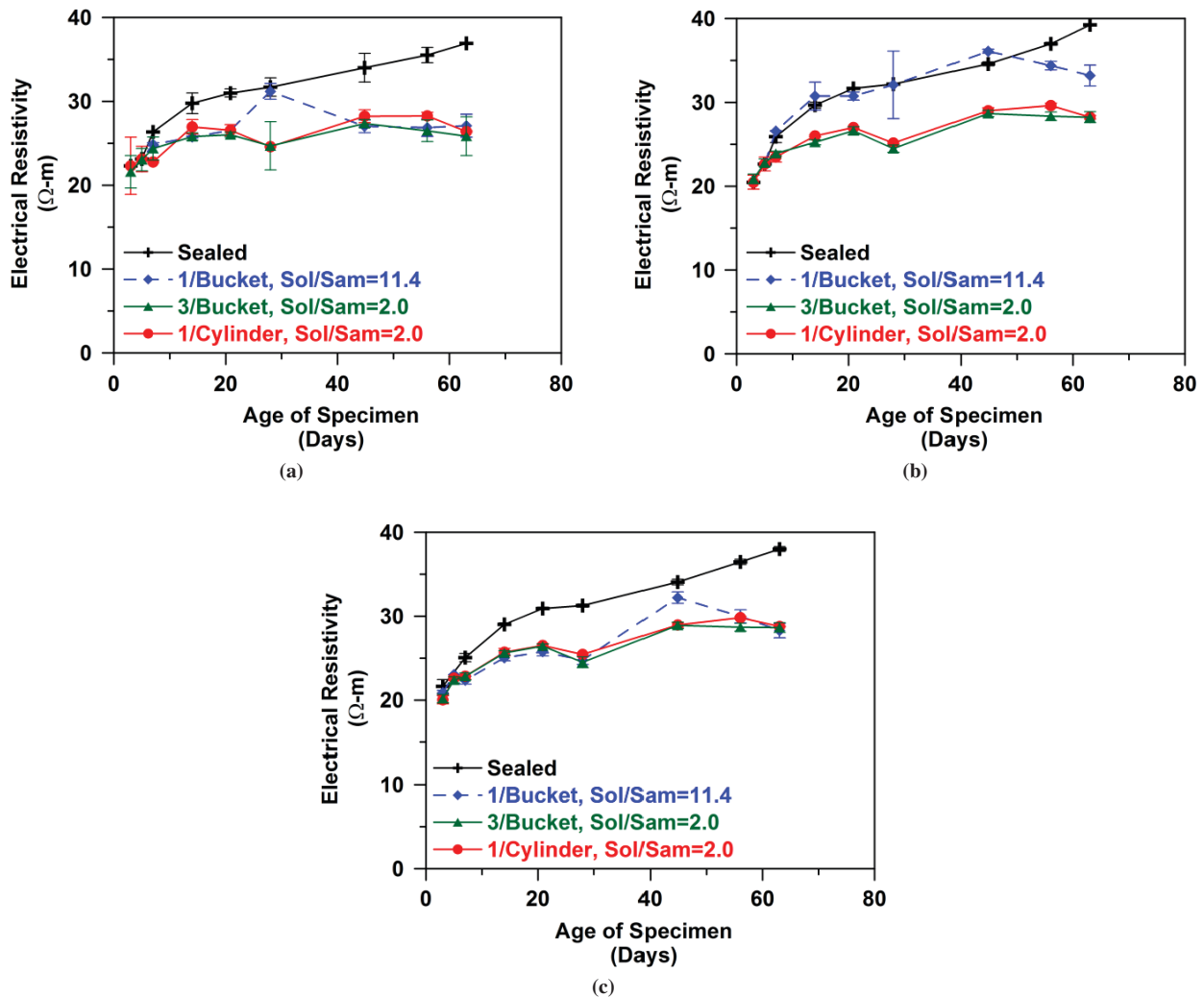


FIGURE 6 Resistivity measurements with different Sol/Sam: (a) surface, (b) uniaxial 40-kHz frequency, and (c) uniaxial multifrequency (error bars represent standard deviation of minimum of three specimens).

generally within the variability of the measurement, but uniaxial measurements at fixed frequencies show differences from 10% to 30% between storage solutions (Figure 6b).

Influence of Measurement Frequency on Total Impedance

Because saturated cementitious systems behave like resistor–capacitor circuits, resulting in a phase difference between the applied current and the measured voltage (impedance), and there is a noticeable difference in impedance at different frequencies, it follows that the real component of the impedance at zero phase angle is the true uniaxial resistance. Because the phase is almost never zero, the meters report the total impedance Z_0 ; the real and imaginary components added in quadrature. To compare the responses of the different meters, an electrical circuit was used. Responses are shown in Figure 7a; the Proceq was configured for uniaxial resistivity. The Solatron meter provided a response over a wide range of frequencies; the values are shown using circular symbols (every 10th symbol is shown). The Miller and Proceq meters were tested at a single frequency and are shown by the triangle- and diamond-shaped symbols, respectively. The phase angle, shown with hollow points and dashed lines, is used to highlight the frequency dependence. Although the measured response of the meters shown in Figure 7a compare well with one another, the data demonstrate why the resistance reported from each unit will not be the same, as they are measured at different frequencies.

The frequency dependence of the electrical response also existed in the uniaxial mortar specimens, as shown for a specimen stored in Sol/Sam of 2.0 at an age of 45 days (Figure 7b). Although there was no significant difference between the measurements of the single-frequency meters and the impedance spectra, a difference is seen in the resistivity that would be reported among these different meters. This difference can be explained through the influence of frequency. Although the two fixed meters operate in the range of 80 to 100 Hz, the measurements used by the Solatron have the lowest imaginary impedance at 794 Hz, which would be the measurement at which the uniaxial resistance would be reported. Note that the Proceq and Miller devices report values approximately 5% lower than the true uniaxial value determined by the Solatron.

A variable frequency was also used to interpret uniaxial resistivity measurements for samples stored using different sample-to-solution volumes. The frequency responses changed as the specimens aged, as shown in Figure 8 for 5- and 65-day samples. Specimens with a larger Sol/Sam exhibited more variability between samples, which was even more pronounced at later ages. This increased variability may be explained by the impedance response across the frequency range. The variability is especially evident in the phase angle measurements, in which the larger storage volume appears to have two local minima (in contrast with the other specimen conditions), which were largely pronounced at later ages, but can be seen as early as 5 days.

CONCLUSIONS

Several key factors should be considered in standardizing tests for the electrical resistivity of cement-based materials. First, different specimen geometries can be used; however, the measured resistance should be converted to resistivity by using an appropriate geometry correction factor. Second, because the temperature of the specimen during the test can influence resistivity measurements, a relatively narrow temperature range (e.g., $\pm 2^\circ\text{C}$) of the test specimens should be specified in standard test methods. The temperature dependence can be partially attributed to the increased mobility of the ionic species of the pore solution. It was shown that both pore solution resistivity and specimen resistivity measurements follow an Arrhenius relationship, with different activation energies of conduction ($E_{A\text{-cond}}$). Third, sample storage and conditioning are also important, as they can influence the degree of hydration, the degree of saturation, and the pore structure and solution through leaching. Differences in resistivity can develop as a result of sample storage conditions (sealed versus saturated). It was observed that when hardened specimens were stored in different solutions of different volumes, inconsistent results were obtained. This inconsistency appears to be related to pore solution dilution, which appears to alter the measured frequency spectra. Testing at variable frequencies can reduce these effects, but for testing at a fixed frequency the solution volume surrounding the sample should be tightly controlled. A solution-to-sample volume ratio of 2.0 appears to be an appropriate recommendation at this time. Studies are underway to investigate this potential

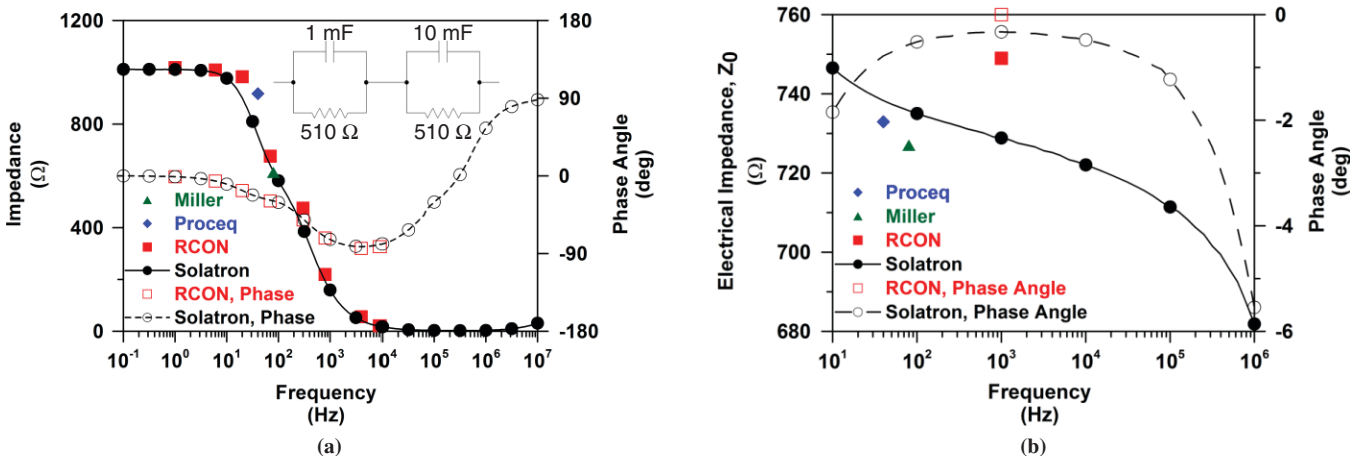


FIGURE 7 Influence of frequency on total impedance illustrated by (a) equivalent circuit and (b) uniaxial measurement on mortar cylinder at age 45 days (deg = degrees).

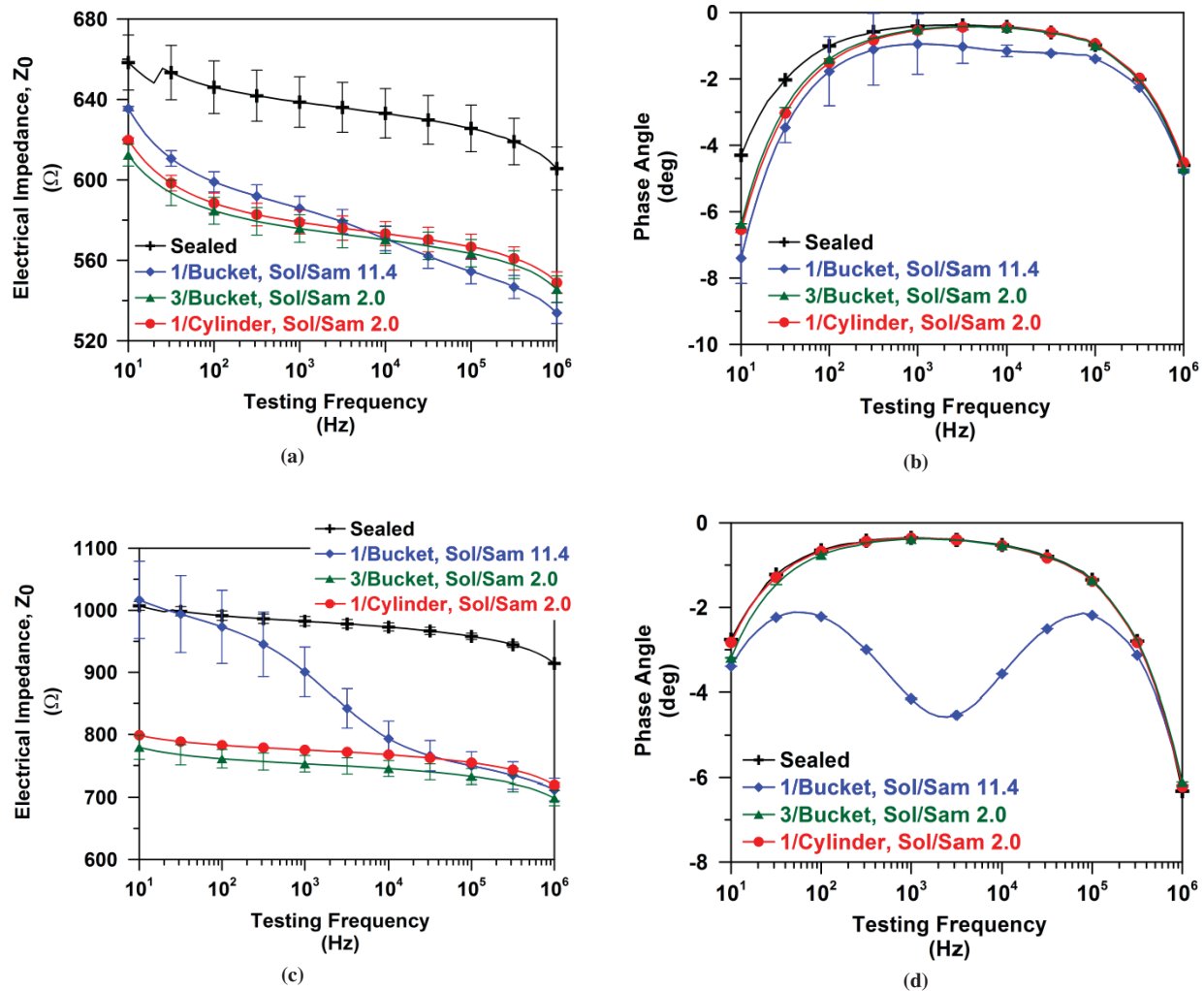


FIGURE 8 Frequency and phase angle responses of specimens with different Sol/Sam at (a) and (b) 5 days and (c) and (d) 65 days (error bars represent standard deviation of three specimens).

dilution effect and the potential gradients that develop in the material that can lead to sample inhomogeneity (36).

ACKNOWLEDGMENTS

This work was supported in part by the Joint Transportation Research Program administered by the Indiana Department of Transportation and Purdue University. The authors thank Giatic Scientific for supplying a unit for testing.

REFERENCES

- Shimizu, Y. An Electrical Method for Measuring the Setting Time of Portland Cement. *Mill Section of Concrete*, Vol. 32, No. 5, 1928, pp. 111–113.
- Calleja, J. Effect of Current Frequency on Measurement of Electrical Resistance of Cement Pastes. *Journal of the American Concrete Institute*, Vol. 24, No. 4, 1952, pp. 329–332.
- Whittington, H. W., J. McCarter, and M. C. Forde. The Conduction of Electricity Through Concrete. *Magazine of Concrete Research*, Vol. 33, No. 114, 1981, pp. 48–60.
- Julio-Betancourt, G. A., and R. D. Hooton. Study of the Joule Effect on Rapid Chloride Permeability Values and Evaluation of Related Electrical Properties of Concretes. *Cement and Concrete Research*, Vol. 34, No. 6, 2004, pp. 1007–1015.
- Snyder, K. A., C. Ferraris, N. S. Martys, and E. J. Garboczi. Using Impedance Spectroscopy to Assess the Viability of the Rapid Chloride Test for Determining Concrete Conductivity. *Journal of Research of the National Institute of Standards and Technology*, Vol. 105, No. 4, 2000, pp. 497–509.
- Rupnow, T. D., and P. Icenogle. *Evaluation of Surface Resistivity Measurements As an Alternative to the Rapid Chloride Permeability Test for Quality Assurance and Acceptance*. Publication FHWA/LA.11/479. Federal Highway Administration, 2011.
- Spragg, R. P., J. Weiss, and T. Nantung. *Proposal for the Development of a Resistivity Method for the Indiana Department of Transportation*. 2012.
- Paredes, M., N. M. Jackson, A. El Safty, J. Dryden, J. Josen, H. Lerma, and J. Hersey. Precision Statements for the Surface Resistivity of Water-Cured Concrete Cylinders in the Laboratory. *Advances in Civil Engineering Materials*, Vol. 1, No. 1, 2012.
- Spragg, R. P., J. Castro, T. Nantung, M. Paredes, and J. Weiss. Variability Analysis of the Bulk Resistivity Measured Using Concrete Cylinders. *Advances in Civil Engineering Materials*, Vol. 1, No. 1, 2012.
- Christensen, B. J., R. T. Coverdale, R. A. Olson, S. J. Ford, E. J. Garboczi, H. M. Jennings, and T. O. Mason. Impedance Spectroscopy of Hydrating Cement-Based Materials: Measurement, Interpretation, and Application. *Journal of the American Ceramic Society*, Vol. 77, No. 11, 1994, pp. 2789–2804.

11. Rajabipour, F. *In Situ Electrical Sensing and Material Health Monitoring in Concrete Structures*. PhD dissertation. Purdue University, West Lafayette, Ind., 2006.
12. Archie, G. E. The Electrical Resistivity Log As an Aid in Determining Some Reservoir Characteristics. *SPE Reprint Series*, 2003, pp. 9–16.
13. Garboczi, E. J. Permeability, Diffusivity, and Microstructural Parameters: A Critical Review. *Cement and Concrete Research*, Vol. 20, No. 4, 1990, pp. 591–601.
14. Snyder, K. A. The Relationship Between the Formation Factor and the Diffusion Coefficient of Porous Materials Saturated with Concentrated Electrolytes: Theoretical and Experimental Considerations. *Concrete Science and Engineering*, Vol. 3, No. 12, 2001, pp. 216–224.
15. McLachlan, D. S., M. Blaszkiewicz, and R. E. Newnham. Electrical Resistivity of Composites. *Journal of the American Ceramic Society*, Vol. 73, No. 8, 1990, pp. 2187–2203.
16. Xie, P., P. Gu, A. Zu, and J. J. Beaudoin. A Rationalized A.C. Impedance Model for the Microstructural Characterization of Hydrating Cement Systems. *Cement and Concrete Research*, Vol. 23, No. 2, 1992, pp. 359–367.
17. Castro, J., R. Spragg, P. Kompare, and W. J. Weiss. *Portland Cement Concrete Pavement Permeability Performance*. Publication FHWA/IN/JTRP-2010/29. Federal Highway Administration, 2010.
18. Morris, W., E. I. Moreno, and A. A. Sagues. Practical Evaluation of Resistivity of Concrete in Test Cylinders Using a Wenner Array Probe. *Cement and Concrete Research*, Vol. 26, No. 12, 1996, pp. 1779–1787.
19. Castro, J., R. Spragg, and J. Weiss. Water Absorption and Electrical Conductivity for Internally Cured Mortars with a W/C Between 0.30 and 0.45. *Journal of Materials in Civil Engineering*, Vol. 24, No. 2, pp. 223–231.
20. Peled, A., J. M. Torrents, T. O. Mason, S. P. Shah, and E. J. Garboczi. Electrical Impedance Spectra to Monitor Damage. *ACI Materials Journal*, Vol. 98, No. 4, 2001, pp. 313–322.
21. Weiss, W. J. *Prediction of Early-Age Shrinkage Cracking in Concrete Elements*. PhD dissertation. Northwestern University, Evanston, Ill., 1999.
22. Hammond, E., and T. D. Robson. Comparison of Electrical Properties of Various Cements and Concretes. *The Engineer*, Vol. 199, 1955, pp. 78–80.
23. McCarter, W. J., G. Starrs, and T. M. Chrisp. Electrical Conductivity, Diffusion, and Permeability of Portland Cement-Based Mortars. *Cement and Concrete Research*, Vol. 30, No. 9, 2000, pp. 1395–1400.
24. Nokken, M., A. Boddy, X. Wu, and R. D. Hooton. Effects of Temperature, Chemical, and Mineral Admixtures on the Electrical Conductivity of Concrete. *Journal of ASTM International*, Vol. 5, No. 5, 2008.
25. Sant, G., F. Rajabipour, and J. Weiss. The Influence of Temperature on Electrical Conductivity Measurements and Maturity Predictions in Cementitious Materials During Hydration. *Indian Concrete Journal*, Vol. 82, 2008, pp. 7–16.
26. Bullard, J. W., C. F. Ferraris, E. J. Garboczi, N. S. Martys, P. E. Stutzman, and J. E. Terrill. Virtual Cement and Concrete. In *Innovations in Portland Cement Manufacturing*, Portland Cement Association, Skokie, Ill., 2008.
27. Weiss, W. J., K. A. Snyder, J. W. Bullard, and D. P. Bentz. Using a Saturation Function to Interpret the Electrical Properties of Partially Saturated Concrete. *Journal of Materials in Civil Engineering*, 2012.
28. Taylor, H. F. W. *Cement Chemistry*. Thomas Telford, London, 1997.
29. Fukuhara, M., S. Goto, K. Asaga, M. Daimon, and R. Kondo. Mechanisms and Kinetics of C₄AF Hydration with Gypsum. *Cement and Concrete Research*, Vol. 11, No. 3, 1981, pp. 407–414.
30. Castro, J. *Moisture Transport in Cement-Based Materials: Application to Transport Tests and Internal Curing*. PhD dissertation. Purdue University, West Lafayette, Ind., 2011.
31. Feng, X., E. J. Garboczi, J. W. Bullard, D. P. Bentz, K. A. Snyder, P. E. Stutzman, and T. O. Mason. *Expanding a Tool for Predicting Chloride Diffusivity in Concrete So It Can Be Used by Manufacturers to Evaluate the Durability of Concrete Made with Blended Cements. Part I: Characterizing Blended Cement Materials. Final Report*. NISTIR 7135. National Institute of Standards and Technology, U.S. Department of Commerce, 2004.
32. Penko, M. *Some Early Hydration Processes in Cement Pastes As Monitored by Liquid Phase Composition Measurements*. Purdue University, West Lafayette, Ind., 1983.
33. Barneyback, S., and S. Diamond. Expression and Analysis of Pore Fluids from Hardened Cement Pastes and Mortars. *Cement and Concrete Research*, Vol. 11, No. 2, 1981, pp. 279–285.
34. Snyder, K. A., X. Feng, B. D. Keen, and T. O. Mason. Estimating the Electrical Conductivity of Cement Paste Pore Solutions from OH, K, and Na Concentrations. *Cement and Concrete Research*, Vol. 33, No. 6, 2003, pp. 793–798.
35. Bentz, D. P. A Virtual Rapid Chloride Permeability Test. *Cement and Concrete Composites*, Vol. 29, No. 10, 2007, pp. 723–731.
36. Spragg, R. P. *The Rapid Assessment of Transport Properties of Cementitious Materials Using Electrical Methods*. MS thesis. Purdue University, West Lafayette, Ind., 2013.

The contents of this paper reflect the views of the authors, who are responsible for the facts and the accuracy of the data presented, and do not necessarily reflect the official views or policies of the Federal Highway Administration and the Indiana Department of Transportation, nor do the contents constitute a standard, specification, or regulation. Certain commercial products are identified in this paper to specify the materials used and procedures employed. In no case does such identification imply endorsement or recommendation by the National Institute of Standards and Technology or Purdue University, nor does it indicate that the products are necessarily the best available for the purpose.

The Durability of Concrete Committee peer-reviewed this paper.